

Long-range Response in AC Electricity Grids

Daniel Jung* and Stefan Kettemann†

Department of Physics & Earth Sciences, Focus Area Health,
Jacobs University Bremen, 28759 Bremen, Germany

(Dated: February 5, 2020)

Local changes in the topology of electricity grids can cause overloads far away from the disturbance [1], making the prediction of the robustness against changes in the topology – for example caused by power outages or grid extensions – a challenging task. The impact of single-line additions on the long-range response of DC electricity grids has recently been studied [2]. By solving the real part of the static AC load flow equations, we conduct a similar investigation for AC grids. In a regular 2D grid graph with cyclic boundary conditions, we find a power law decay for the change of power flow as a function of distance to the disturbance over a wide range of distances. The power exponent increases and saturates for large system sizes. By applying the same analysis to the German transmission grid topology, we show that also in real-world topologies a long-ranged response can be found.

PACS numbers: 88.80.H-, 88.80.hm, 88.80.hh, 84.70.+p,

Power grids provide electrical power to billions of individuals reliably. For example, in Germany the average outage time experienced by a consumer in 2006 was 20 minutes and continued to decrease in the last decade to 12.5 minutes in 2014 [3]. Still, the energy transition towards an increased supply of decentralized renewable energy raises concerns that the change from the previously centralised power production with unidirectional power flow towards a decentralised electrical power system with bidirectional flow might be harmful for the stability of electricity grids. Disturbances and power outages might spread more easily in highly connected grids and cause nonlocal disturbances, which may cause larger instabilities of the entire grid. Therefore, it is essential to get a better understanding of the physical mechanisms leading to nonlocal disturbances and how their spreading depends on the connectivity and topology of the grid.

In a previous work, the long-range response to the addition of another transmission line for the case of a DC grid including losses by Joule heating has been studied [2]. It has been demonstrated that the absolute change of transmitted power as function of the distance to the perturbation follows a power law. Real power transmission grids usually use three-phasic alternating current (AC) [4]. Hence, we are going to perform a similar analysis for AC networks.

An electrical power transmission system can formally be described as a (multi)graph G that consists of nodes $i, j \in \mathcal{N}$ (substations) and edges $(i, j) \in \mathcal{E}$ (transmission lines), where \mathcal{N} is the set of all nodes and \mathcal{E} the set of all edges of G . The network model gains its physical meaning by defining appropriate node and edge attributes. Starting from the *Kirchhoff's laws* and *Ohm's law*, it is straightforward to write down the *steady state power flow equations* for a three-phase AC network,

$$S_i - 3V_i \sum_j Y_{ij}^* (V_i - V_j)^* = 0 \quad , \quad (1)$$

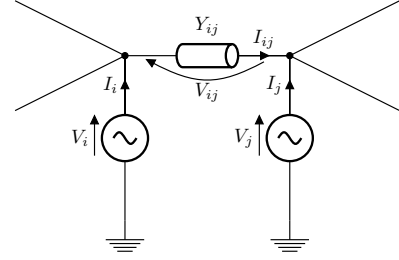


FIG. 1. Sketch of a section of an electricity grid with a transmission line connecting nodes (i, j) with admittance Y_{ij} , carrying a current I_{ij} at voltages V_i and V_j .

where the three alternating currents of the same frequency are phase shifted by 120 degrees. Here, $S_i = P_i + iQ_i$ is the *net generated power* entering the network at node i (negative for a consumer, positive for a generator), and V_i is the terminal voltage of the machine connected at node i . Y_{ij} is the admittance of the transmission line (i, j) [5]. For a transmission line in an arbitrary AC network, the labeling is illustrated in Fig. 1.

If we restrict ourselves to a purely inductive grid (no Joule heating),

$$Y_{ij} = \frac{1}{i\omega L_{ij}} \quad , \quad (2)$$

we can assume sinusoidal voltages with a constant magnitude $|V_i| \equiv V$ [6],

$$V_i(\omega, t) = V e^{i\varphi_i(\omega, t)} \quad , \quad (3)$$

with phase angles $\varphi_i(\omega, t) = \omega t + \theta_i(t)$. Thus only the phase difference between adjacent nodes can give rise for an electrical current. We are looking for steady states with constant grid frequency ω (e.g. $\omega = 2\pi \cdot 50$ Hz). The *power capacity* of a transmission line (a set of three

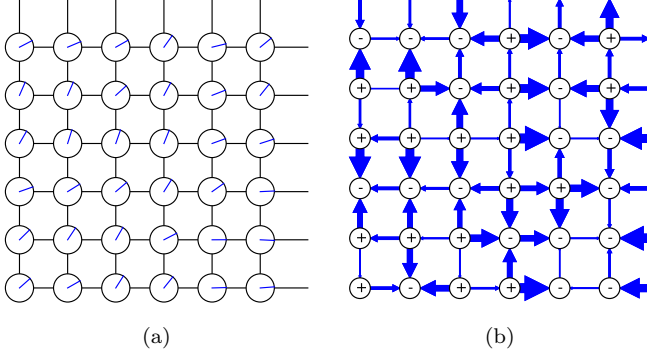


FIG. 2. (a) Voltage phase distribution of an example system with binary distribution of the net generated power $P_i \in \{-P, P\}$ at each node. (b) The respective power flow transmitted through each transmission line. The size of the arrows is proportional to the transmitted power F_{ij} . The symbols “+” and “-” indicate generators and consumers, respectively.

wires) is given by

$$K_{ij} = \frac{3V^2}{\omega L_{ij}} . \quad (4)$$

So the power flow equations (1) become

$$S_i = i \sum_j K_{ij} \left(1 - e^{i(\theta_i - \theta_j)}\right) . \quad (5)$$

The real part gives the balance of the *active power* flow,

$$P_i = \sum_j K_{ij} \sin(\theta_i - \theta_j), \quad (6)$$

which determines the phases θ_i at all nodes for given power P_i . The imaginary part of Eq. (5) gives the balance of the *reactive power* Q_i . For the constant voltage amplitudes considered in this article, the N active power equations determine the N phases φ_i which fix the reactive power at node i , Q_i .

If there exists a stationary solution θ_i for the chosen system parameters, it can easily be found using some standard root-finding algorithm [7], see Fig. 2a for an example. Given a solution for the phase distribution θ_i , the transmitted power F_{ij} from node i to node j is given by

$$F_{ij} = K_{ij} \sin(\theta_i - \theta_j) \quad , \quad (7)$$

as plotted in Fig. 2b, where the thickness of the arrows is proportional to $|F_{ij}|$.

Then we add a single line to the graph and calculate the modified transmitted powers F'_{ij} (see Fig. 3a). We then calculate the difference $\Delta F_{ij} = F'_{ij} - F_{ij}$ and study the average absolute difference $\langle |\Delta F_{ij}| \rangle$ of all edges as a function of their distance to the added line (see Fig. 3b). The average covers all edges with the same distance r

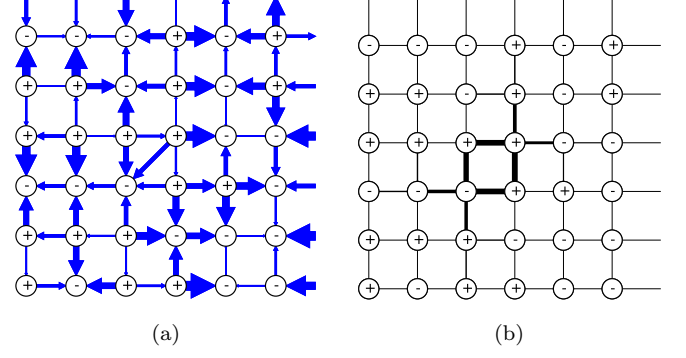


FIG. 3. (a) Power flow of the same system as in Fig. 2 after the addition of another transmission line. (b) Absolute change of the power flows $|\Delta F_{ij}|$ in the original grid after adding the line. The width of the lines is proportional to $|\Delta F_{ij}|$.

to the added line as well as an ensemble average over $R = 1000$ disorder realizations (random distributions for the P_i).

We first consider a regular 2D grid graph of linear size L with cyclic boundary conditions, so the system size (number of nodes) is given by $N = L^2$. In this graph it is particularly simple to define a measure for the distance between two edges by counting the number of edges that have to be passed (shortest path), as illustrated in Fig. 4. We further consider a binary distribution for the nodal *net generated power* P_i , where nodes with $P_i = +P$ are regarded as generators and nodes with $P_i = -P$ as consumers. We set the power capacity of all lines to $K_{ij} = K$, so we can note down all power quantities in units of K . In order to find a stable solution, the condition $\sum_i P_i = 0$ must be fulfilled at all times, which rules out the possibility of odd linear sizes L .

In order to precisely control the amount of disorder in the system, we use the following procedure to generate a random distribution of the P_i : We start from a periodic arrangement of generators and consumers [11] and divide the graph into two subgraphs, one carrying all $N/2$ generators and the other all $N/2$ consumers. Then, p different nodes are chosen randomly from each subgraph, forming p generator-consumer pairs. Finally, each of these generator-consumer pairs is swapped. By generating a permutation of the periodic arrangement in this way, it is ensured that no node is swapped twice, and the amount of disorder $w \in [0, 1]$ is precisely defined as

$$w = \frac{4p}{N} \quad , \quad (8)$$

depending on the number of swapped generator-consumer pairs p . The maximally disordered state is reached after $p_{\max} = N/4$ swaps. There is a finite number of possible realizations, given by the ensemble size

$$N_E = \binom{N/2}{p} \quad , \quad (9)$$

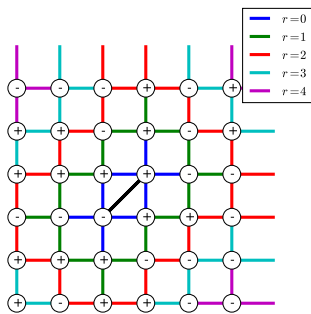


FIG. 4. (Color online) Classification of the transmission lines by their distance r to the added line (black).

which is however very large for the considered system sizes.

To study the long-range response of the grid to the added transmission line, we classify all edges of the graph by their distance r to the new edge by counting the number of edges that link the considered edge to the new edge (see Fig. 4 for an illustration). We average the change in the amplitude of the transmitted power $|\Delta F_{ij}|$ over all edges with the same distance r to the added line, and perform an ensemble average $\langle |\Delta F_{ij}| \rangle(r)$ over $R = 1000$ realizations with the same disorder strength w . Realizations for which no steady state solution can be found are skipped. This happens in particular if the transmitted power F_{ij} is exceeding the capacity K_{ij} of at least one transmission line (i, j) so that Eq. (7) cannot be fulfilled since $\sin(\theta_i - \theta_j) > F_{ij}/K_{ij}$. For the square grid, the power capacity K has to exceed the critical value $K_c = P/4$ in order to obtain a steady state power flow at all [12]. Since for a random arrangement of P_i larger clusters of N_c generators or consumers can occur with total power $N_c P$, the lines connected to these clusters can be overloaded even if the power capacity exceeds the critical value $K > K_c$, and no steady state solution is found. Thus, only a certain subset of realizations leads to a solution for the θ_i .

$\langle |\Delta F_{ij}| \rangle(r)$ has been calculated for different linear system sizes L and plotted on a double-logarithmic scale in Fig. 5. Up to a certain distance r_{sat} , $\langle |\Delta F_{ij}| \rangle$ is a steadily decreasing function of r . The value r_{sat} is found to depend on system size L . For distances r exceeding r_{sat} (region R4), the data saturates, or even a small increase is noticeable, which is probably an effect caused by the cyclic boundary conditions. For distances $r < r_{\text{sat}}$ we are able to identify two regimes R1 and R2 that both show a power-law-like behavior of $\langle |\Delta F_{ij}| \rangle(r)$, but with different power exponents b . Beyond R2, close to r_{sat} , there is a region where the data deviates somewhat from a pure power law behavior (region R3).

For the regimes R1 and R2 we fit the data to a power law, using the fit model

$$f(r) = ar^{-b} \quad . \quad (10)$$

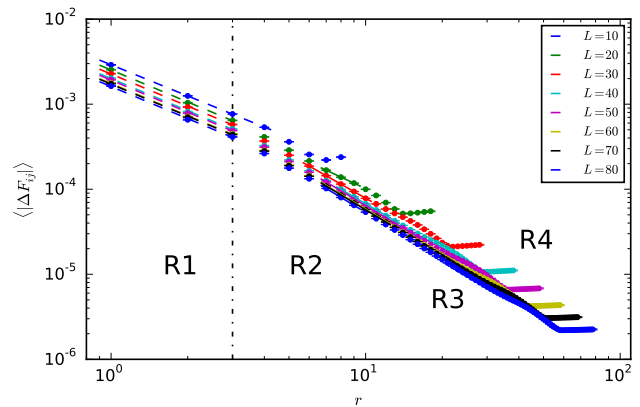


FIG. 5. (Color online) Double-logarithmic plot of $\langle |\Delta F_{ij}| \rangle(r)$ for different system sizes L and $P/K = 0.25$. For the regimes R1 and R2, the data has been fitted to a power law. Error bars correspond to 95% confidence intervals.

The fit results are shown in Tab. I (R1) and Tab. II (R2). To assess the quality of the fit, we compute the χ^2 statistic and the goodness of fit probability Q [13]. For each fit, we choose an optimal range $(r_{\text{min}}, r_{\text{max}})$ so that Q is closest to 0.5. Thus, the number of considered data points is $N_D = r_{\text{max}} - r_{\text{min}} + 1$. For the error bars, 95% confidence intervals are considered.

Due to the small number of data points at small distances r , the fit quality in regime R1 is not acceptable. Thus, we are not able to quantitatively prove the existence of a power law in regime R1, despite the qualitative indications.

In regime R2, there are more data points (increasing with system size), since the number of nodes at a certain distance r increases with distance, so the standard error becomes smaller. The fit quality is found to be mostly optimal and the power exponent b can be determined with high accuracy. Thus, we find clear evidence that the reaction of an AC power transmission grid to a local modification of the topology is of long-ranged nature, decaying with a power law with distance r with exponent b .

In Fig. 6, we analyze the system size dependence of the power exponent b in regime R2. The data suggests a saturation of b in the limit of large system sizes. We find the largest $b = 1.812 \pm 0.017$ for a linear system size of $L = 80$, when the power is set to $P/K = 0.25$. Remarkably, we do not find a significant dependence of the power exponent b on the ratio P/K for these system sizes. A dependence on P/K could have been expected, since the larger P/K , the smaller are the allowed changes ΔF_{ij} when adding the additional transmission line. Therefore, one could have expected that the response becomes more long-ranged, corresponding to smaller powers b , when increasing P/K . However, no such tendency can be confirmed for the studied P/K ratios. We note here that we fixed the amount of disorder in the system to the maxi-

TABLE I. Fit results for regime R1. For each parameter combination (P, L) , only data for $r_{\min} \leq r \leq r_{\max}$ is considered. To assess the quality of the fit, χ^2 and the quality of fit probability Q are given.

P/K	L	r_{\min}	r_{\max}	a	b	χ^2	Q
0.0625	10	1	4	0.000716 ± 0.000004	1.218 ± 0.005	2.60	0.27
	20	1	3	0.000657 ± 0.000014	1.251 ± 0.027	17.67	10^{-5}
	30	1	3	0.000580 ± 0.000017	1.253 ± 0.035	30.71	10^{-8}
	40	1	3	0.000513 ± 0.000016	1.253 ± 0.038	35.50	10^{-9}
	50	1	3	0.000492 ± 0.000016	1.253 ± 0.040	38.51	10^{-9}
	60	1	3	0.000441 ± 0.000015	1.253 ± 0.041	36.58	10^{-9}
	70	1	3	0.000417 ± 0.000014	1.253 ± 0.041	36.99	10^{-9}
	80	1	3	0.000434 ± 0.000015	1.253 ± 0.042	36.31	10^{-9}
0.1250	10	1	4	0.001534 ± 0.000008	1.218 ± 0.005	2.78	0.25
	20	1	3	0.001191 ± 0.000026	1.250 ± 0.027	16.89	10^{-4}
	30	1	3	0.001159 ± 0.000034	1.252 ± 0.035	29.45	10^{-7}
	40	1	3	0.001054 ± 0.000033	1.253 ± 0.038	34.00	10^{-8}
	50	1	3	0.000965 ± 0.000032	1.253 ± 0.040	37.53	10^{-9}
	60	1	3	0.000910 ± 0.000031	1.253 ± 0.041	37.24	10^{-9}
	70	1	3	0.000823 ± 0.000028	1.253 ± 0.041	38.66	10^{-9}
	80	1	3	0.000840 ± 0.000029	1.253 ± 0.041	39.98	10^{-10}
0.2500	10	1	4	0.002906 ± 0.000015	1.217 ± 0.005	2.46	0.29
	20	1	3	0.002525 ± 0.000055	1.250 ± 0.026	17.88	10^{-5}
	30	1	3	0.002261 ± 0.000066	1.252 ± 0.035	29.38	10^{-7}
	40	1	3	0.001999 ± 0.000063	1.253 ± 0.038	33.85	10^{-8}
	50	1	3	0.001919 ± 0.000063	1.253 ± 0.039	37.32	10^{-9}
	60	1	3	0.001755 ± 0.000059	1.253 ± 0.040	38.27	10^{-9}
	70	1	3	0.001722 ± 0.000059	1.253 ± 0.041	39.55	10^{-9}
	80	1	3	0.001612 ± 0.000056	1.253 ± 0.042	34.97	10^{-8}
0.5000	10	1	4	0.005726 ± 0.000031	1.217 ± 0.005	2.58	0.27
	20	1	3	0.005108 ± 0.000110	1.249 ± 0.026	16.10	10^{-4}
	30	1	3	0.004502 ± 0.000129	1.252 ± 0.034	26.67	10^{-7}
	40	1	3	0.004087 ± 0.000127	1.252 ± 0.037	33.63	10^{-8}
	50	1	3	0.004112 ± 0.000133	1.252 ± 0.039	34.76	10^{-8}
	60	1	3	0.003576 ± 0.000119	1.253 ± 0.040	35.69	10^{-9}
	70	1	3	0.003428 ± 0.000116	1.252 ± 0.041	36.09	10^{-9}
	80	1	3	0.003446 ± 0.000117	1.253 ± 0.041	38.00	10^{-9}
1.0000	10	1	3	0.011690 ± 0.000043	1.205 ± 0.004	0.53	0.47
	20	1	3	0.010237 ± 0.000119	1.248 ± 0.014	4.79	0.03
	30	1	3	0.009107 ± 0.000184	1.250 ± 0.024	14.71	10^{-4}
	40	1	3	0.008132 ± 0.000195	1.251 ± 0.029	19.64	10^{-5}
	50	1	3	0.007796 ± 0.000195	1.248 ± 0.030	20.32	10^{-5}
	60	1	3	0.007497 ± 0.000203	1.249 ± 0.033	22.12	10^{-6}
	70	1	3	0.007071 ± 0.000207	1.250 ± 0.035	28.17	10^{-7}
	80	1	3	0.006430 ± 0.000189	1.251 ± 0.035	28.23	10^{-7}

mal value $w = 1$.

In contrast to the power exponent b , the preexponential a in Eq. (10) increases with P/K linearly, as shown in Fig. 7. This behavior is expected, since the addition of a transmission line with power capacity K will lead to a redistribution of the power flow in proportion to the generated power P/K , so that $\langle |\Delta F_{ij}| \rangle \sim P/K$ is expected

on average.

We also analyze the value of $\langle |\Delta F_{ij}| \rangle(r)$ as function of system size L for the smallest distance $r = 0$, the largest distance $r = L - 2$ and at the value $r = r_{\text{sat}}$, where $\langle |\Delta F_{ij}| \rangle$ starts to saturate, as shown in Fig. 8. The dependence on L is qualitatively following a power law, $g(L) = e + cL^{-d}$. The fit results are summarized in

TABLE II. Fit results for regime R2. For each parameter combination (P, L) , only data for $r_{\min} \leq r \leq r_{\max}$ is considered. To assess the quality of the fit, χ^2 and the quality of fit probability Q are given.

P/K	L	r_{\min}	r_{\max}	N_D	a	b	χ^2	Q
0.0625	20	7	9	3	0.000659 ± 0.000020	1.396 ± 0.014	0.79	0.37
	30	6	10	5	0.001021 ± 0.000014	1.706 ± 0.007	2.58	0.46
	40	8	13	6	0.000996 ± 0.000014	1.760 ± 0.006	3.32	0.51
	50	7	16	10	0.001026 ± 0.000008	1.795 ± 0.003	7.36	0.50
	60	7	12	6	0.000924 ± 0.000014	1.799 ± 0.007	4.29	0.37
	70	7	12	6	0.000883 ± 0.000014	1.804 ± 0.007	4.46	0.35
	80	7	9	3	0.000933 ± 0.000033	1.812 ± 0.017	0.97	0.33
	0.1250	20	7	9	3	0.001193 ± 0.000036	1.396 ± 0.014	0.75
30		6	10	5	0.002040 ± 0.000028	1.706 ± 0.007	2.47	0.48
40		8	13	6	0.002048 ± 0.000028	1.760 ± 0.006	3.17	0.53
50		7	16	10	0.002010 ± 0.000015	1.795 ± 0.003	7.17	0.52
60		7	12	6	0.001908 ± 0.000028	1.799 ± 0.007	4.37	0.36
70		7	12	6	0.001742 ± 0.000027	1.804 ± 0.007	4.68	0.32
80		8	10	3	0.001647 ± 0.000026	1.769 ± 0.007	0.16	0.69
0.2500		20	7	9	3	0.002531 ± 0.000075	1.396 ± 0.014	0.78
	30	6	10	5	0.003981 ± 0.000055	1.706 ± 0.007	2.44	0.49
	40	8	13	6	0.003884 ± 0.000053	1.760 ± 0.006	3.12	0.54
	50	7	16	10	0.003998 ± 0.000029	1.795 ± 0.003	7.10	0.53
	60	7	12	6	0.003680 ± 0.000055	1.799 ± 0.007	4.52	0.34
	70	7	12	6	0.003645 ± 0.000056	1.804 ± 0.007	4.81	0.31
	80	7	9	3	0.003467 ± 0.000125	1.812 ± 0.017	0.94	0.33
	0.5000	20	7	9	3	0.005128 ± 0.000154	1.396 ± 0.014	0.76
30		7	10	4	0.008047 ± 0.000168	1.712 ± 0.010	1.54	0.46
40		7	12	6	0.008005 ± 0.000106	1.763 ± 0.006	3.66	0.45
50		8	16	9	0.008577 ± 0.000078	1.795 ± 0.004	6.29	0.51
60		7	12	6	0.007501 ± 0.000110	1.799 ± 0.006	4.12	0.39
70		7	12	6	0.007258 ± 0.000110	1.803 ± 0.007	4.35	0.36
80		7	9	3	0.007398 ± 0.000242	1.811 ± 0.016	0.86	0.35
1.0000		20	5	7	3	0.015381 ± 0.000108	1.601 ± 0.004	0.08
	30	6	8	3	0.015940 ± 0.000270	1.700 ± 0.009	0.33	0.56
	40	8	10	3	0.016045 ± 0.000461	1.765 ± 0.013	0.54	0.46
	50	8	11	4	0.016012 ± 0.000359	1.785 ± 0.010	1.39	0.50
	60	8	19	12	0.016522 ± 0.000120	1.818 ± 0.003	9.59	0.48
	70	7	10	4	0.014603 ± 0.000297	1.790 ± 0.009	1.45	0.48
	80	7	9	3	0.013653 ± 0.000388	1.804 ± 0.014	0.64	0.42

Tab. III and visualized in Fig. 8, setting $e = 0$. We find a different power exponent d in the small distance regime at $r = 0$ than in the limit of large distances $r = L - 2$. The low fit quality shows that either the data does not follow a pure power law (with $e = 0$), or that the statistical error of the data (standard error of the mean) has been underestimated.

Having verified the long-range response of local grid modifications in AC electricity grids, a comparison of the results to an earlier study considering long-range response in DC grids [2] is in place. In the DC case also two power-law regimes R1 and R2 have been found, but in

contrast to AC results, the exponent b does not increase but decrease when going from R1 to R2. Also the absolute values of the exponents b are different in AC and DC grids, finding for a linear system size of $L = 50$ in regime R2 $b = 1.32$ [2] for DC and $b = 1.795 \pm 0.003$ for AC.

In order to move towards more realistic grid structures, we show in the following preliminary results using a model for the German transmission grid [15]. To be able to compare to the results for the 2D grid, we only change the topology. All other assumptions stay intact, in particular the constant power capacity $K_{ij} = K$ and

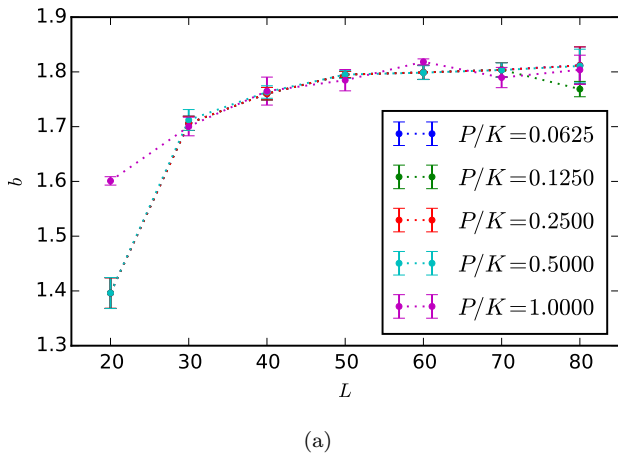


FIG. 6. Dependence of the power exponent b on the linear system size L for different ratios P/K . Error bars correspond to 95% confidence intervals.

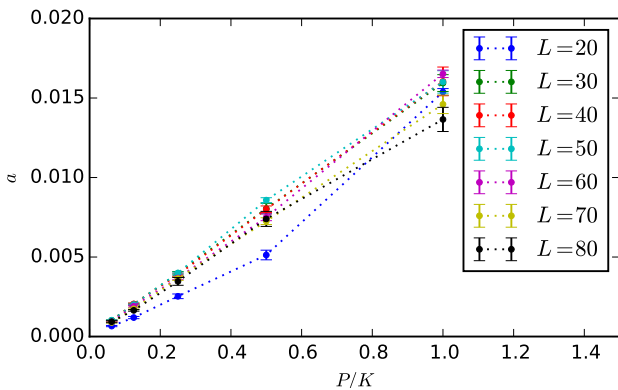


FIG. 7. Dependence of the fit parameter a on the ratio P/K for different linear system sizes L . Error bars correspond to 95% confidence intervals.

the binary generator distribution $P_i \in \{-P, P\}$. Also the distance r to the added line is measured by simply counting edges as before.

The first difference to the 2D grid is that the choice (location) of the added line influences the results, so we have to study different line locations separately. To exemplify this, we add two example lines that connect nodes with a high betweenness centrality c_B , as we think that this choice could lead to results most similar to those of the 2D grid topology. Fig. 9 shows how a single line addition changes the flows throughout the German grid (for a single distribution of generators). Fig. 10 shows the result for the function $\langle |\Delta F_{ij}| \rangle(r)$ for the two added lines. It proves that adding different lines in different locations can lead to both different magnitude and shape of the outgoing response. Remarkably, the values are not monotonically decreasing anymore.

To conclude, we have shown numerically that local grid modifications – in this special case the addition of a single transmission line – cause a long-range response in

TABLE III. (a) Fit results for the finite size scaling of $\langle |\Delta F_{ij}| \rangle(r)$ for $r = 0$ (smallest distance), $r = L - 2$ (largest distance) and $r = r_{\text{sat}}$ (saturation value) as a function of linear system size L . To assess the quality of the fit, χ^2 and the quality of fit probability Q are given.

r	P/K	N_D	c	d	χ^2	Q
0	0.0625	8	0.006 ± 0.001	0.268 ± 0.025	254.2	10^{-51}
0	0.1250	8	0.013 ± 0.001	0.287 ± 0.019	151.6	10^{-29}
0	0.2500	8	0.025 ± 0.001	0.280 ± 0.015	87.4	10^{-16}
0	0.5000	8	0.047 ± 0.003	0.254 ± 0.020	158.5	10^{-31}
0	1.0000	8	0.099 ± 0.006	0.271 ± 0.016	113.2	10^{-21}
$L - 2$	0.0625	8	0.011 ± 0.001	2.237 ± 0.030	430.1	10^{-89}
$L - 2$	0.1250	8	0.023 ± 0.002	2.256 ± 0.021	213.0	10^{-42}
$L - 2$	0.2500	8	0.044 ± 0.003	2.250 ± 0.020	194.1	10^{-38}
$L - 2$	0.5000	8	0.082 ± 0.007	2.223 ± 0.024	274.9	10^{-56}
$L - 2$	1.0000	8	0.178 ± 0.014	2.244 ± 0.022	218.6	10^{-44}
r_{sat}	0.0625	8	0.010 ± 0.001	2.236 ± 0.033	1533.6	0.00
r_{sat}	0.1250	8	0.021 ± 0.002	2.247 ± 0.027	1094.1	10^{-232}
r_{sat}	0.2500	8	0.042 ± 0.003	2.246 ± 0.021	583.0	10^{-122}
r_{sat}	0.5000	8	0.078 ± 0.009	2.220 ± 0.029	1174.5	10^{-250}
r_{sat}	1.0000	8	0.174 ± 0.019	2.247 ± 0.028	1045.2	10^{-222}

AC electricity grids. This finding can also be relevant for other types of perturbations, for example fluctuations in the power production of small, decently placed generators (photovoltaics, wind power), as small changes in the generated power or small phase perturbations can have an impact on the stable operation of a large part of the grid. In a conventional energy grid, the largest consumers (industry) as well as the largest generators usually consist of large rotating masses, so small perturbations are easily smoothed out. As of the energy transition towards an increasingly decentral power generation, generators that do not possess this kind of buffer of electrical energy in form of inertia – namely photovoltaic cells – produce an increasing share of the energy supply. This study should be extended to other topologies like random graphs and in particular real world topologies, eventually also including real line parameters and power distributions. Furthermore, the analysis could be extended to the complete AC power flow equations, including the reactive power Q_i . Ultimately, this approach could lead to quantitative predictions if a particular grid extension measure improves or diminishes the overall stability of the electricity grid.

The numerical calculations have been performed using computational resources of the Computational Laboratories for Analysis, Modeling and Visualization (CLAMV), Jacobs University Bremen, Germany. We gratefully acknowledge support of BMBF, CoNDyNet, FK. 03SF0472A.

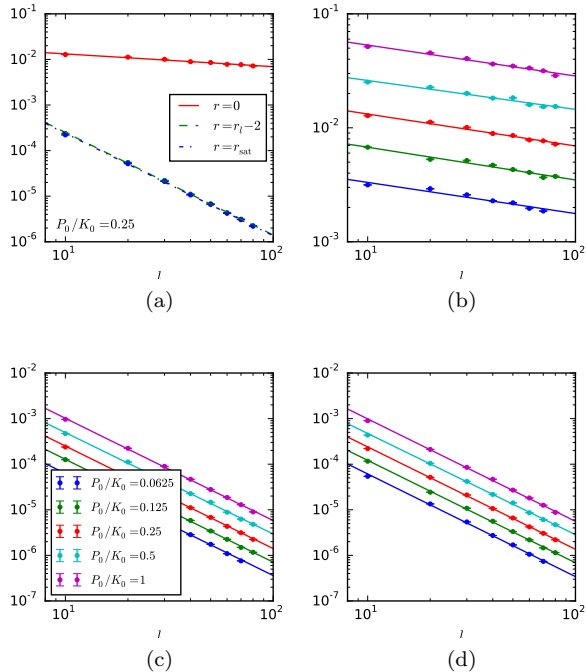


FIG. 8. (Color online) $\langle |\Delta F_{ij}| \rangle(r)$ for (b) $r = 0$ (smallest distance), (c) $r = L - 2$ (largest distance) and (d) $r = r_{\text{sat}}$ (saturation value) as a function of linear system size L . (a) All of the above for $P/K = 0.25$. Error bars correspond to 95 % confidence intervals.

* d.jung@jacobs-university.de

† s.kettemann@jacobs-university.de

- [1] D. Witthaut and M. Timme, The European Physical Journal B **86**, 377 (2013).
- [2] D. Labavić, R. Suciú, H. Meyer-Ortmanns, and S. Kettemann, Eur. Phys. J. Spec. Top. **223**, 2517 (2014).
- [3] Versorgungsqualität – SAIDI-Werte 2006-2014, Bundesnetzagentur (2015).
- [4] K. Heuck, K.-D. Dettmann, and D. Schulz, *Elektrische Energieversorgung*, 9th ed. (Springer Fachmedien Wiesbaden, Wiesbaden, 2013).
- [5] The star symbol (*) denotes the complex conjugate.
- [6] S. Kettemann, Phys. Rev. Lett., to be published, arXiv:1504.05525v2 (2015).
- [7] We use the Python function `scipy.optimize.fsolve` [8, 9], which is a wrapper around the functions `hybrd` and `hybrj` of the Fortran package `MINPACK` [10].
- [8] E. Jones, T. Oliphant, P. Peterson, and others, *SciPy: Open source scientific tools for Python* (2001).
- [9] Travis E. Oliphant. Python for Scientific Computing, Computing in Science & Engineering **9**, 10-20 (2007), DOI:10.1109/MCSE.2007.58
- [10] J. J. Moré, B. S. Garbow, and K. E. Hillstom, *User Guide for MINPACK-1*, Tech. Rep. ANL-80-74 (Argonne National Laboratory, Argonne, IL, USA, 1980).

[11] Similar to the “antiferromagnetic groundstate” known from solid state theory.

[12] For K_c , only a periodic arrangement of generators and

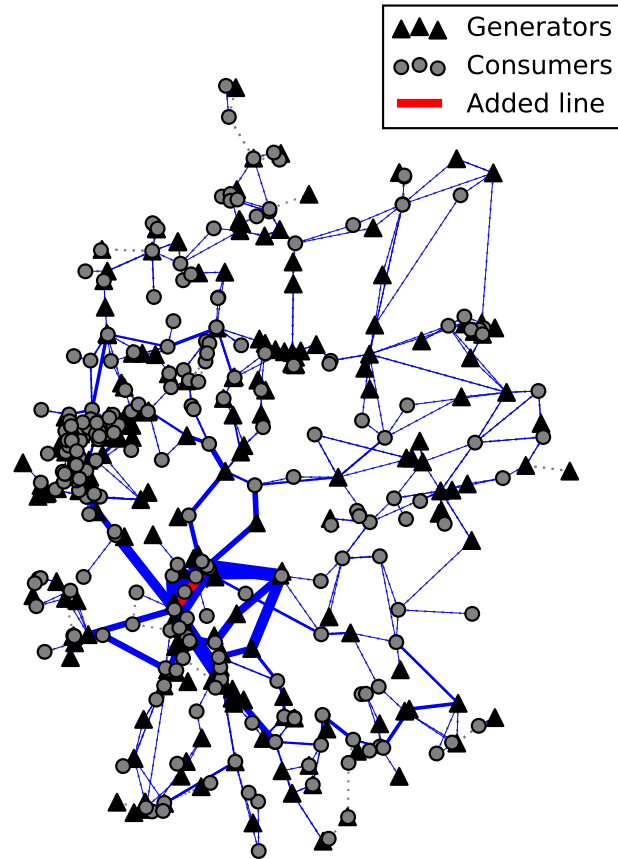


FIG. 9. (Color online) Example of change of power flow $|\Delta F_{ij}|$ in the German grid with binary generator distribution by adding another line. The width of the blue lines is proportional to $|\Delta F_{ij}|$.

consumers remains as realization with a solution.

[13] To assess the quality of the fits, we compute the *goodness of fit probability* (GOF) [14]

$$Q = \int_{x^2}^{\infty} p(x, k) dx \quad , \quad (11)$$

where

$$p(x, k) = \frac{x^{(k-2)/2} e^{-x/2}}{2^{k/2} \Gamma(k/2)} \quad (12)$$

is the *chi-squared distribution* [14] and $k = N_D - N_P$ is the number of *degrees of freedom* (DOF). N_D is the number of data points and N_P the number of fit parameters in the fit model.

[14] P. Bevington and D. K. Robinson, *Data Reduction and Error Analysis for the Physical Sciences*, 3rd ed. (McGraw-Hill Education, Boston, 2002), p. 336.

[15] SciGRID, NEXT ENERGY – EWE Research Centre for Energy Technology, <http://www.scigrid.de/>.

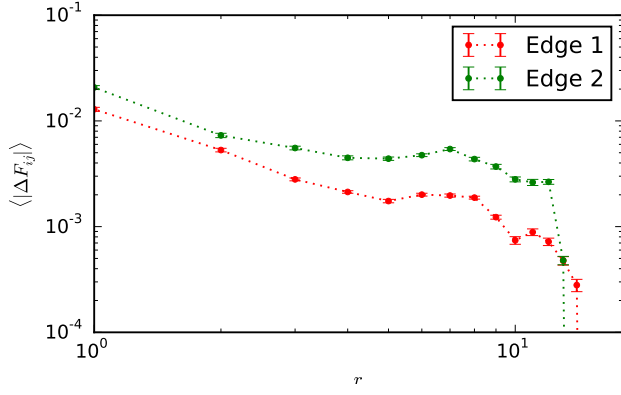


FIG. 10. (Color online) Double-logarithmic plot of $\langle |\Delta F_{ij}^r| \rangle$ for the German transmission grid model with $P/K = 1$, $w = 1$ and $R = 100$. Lines connecting nodes with the highest betweenness centrality c_B have been added. Error bars correspond to 95% confidence intervals.